

Catalytic abatement of volatile organic compounds assisted by non-thermal plasma

Part 1. A novel dielectric barrier discharge reactor containing catalytic electrode

Ch. Subrahmanyam^a, M. Magureanu^b, A. Renken^a, L. Kiwi-Minsker^{a,*}

^a *Ecole Polytechnique Fédérale de Lausanne (LGRC-EPFL), CH-1015 Lausanne, Switzerland*

^b *National Institute for Lasers, Plasma and Radiation Physics, Bucharest, Romania*

Received 10 November 2005; received in revised form 5 January 2006; accepted 16 January 2006

Available online 10 March 2006

Abstract

A novel catalytic reactor with dielectric barrier discharge (DBD) at atmospheric pressure was developed for the abatement of volatile organic compounds (VOCs). The novelty of DBD reactor is the metallic catalyst serving also as the inner electrode. The catalytic electrode was prepared from sintered metal fibers (SMF) in the form of a cylindrical tube. Oxides of Mn and Co were deposited on SMF by impregnation. Decomposition of toluene taken as the model VOC compound (<1000 ppm in air) was investigated. The catalyst composition, toluene concentration, applied voltage and frequency were systematically varied to evaluate the performance of the DBD reactor. At 100 ppm of toluene, the conversion ~100% was achieved in the DBD reactor using a specific input energy (SIE) ~ 235 J/l independently of the chemical composition of the SMF catalytic electrode, but the selectivity to CO₂ was observed to be a function of the catalyst composition. The MnO_x/SMF catalytic electrode showed the best performance towards total oxidation. At a SIE of 295 J/l, the selectivity to CO₂ was 80% with 100% conversion of toluene. No carbon solid residues were deposited on the electrode.

© 2006 Elsevier B.V. All rights reserved.

Keywords: Volatile organic compounds abatement; Non-thermal plasma; Dielectric barrier discharge; Plasma-assisted catalysis; Sintered metal fibers

1. Introduction

The emission of volatile organic compounds (VOCs) into the atmosphere by various industrial and agrochemical processes is an increasing environmental and social concern over the last years. Some of them are carcinogens and cause respiratory disorders. Therefore, the removal of VOCs is an important issue and needs highly efficient low cost processes. Conventional techniques in use for the removal of VOCs mainly include adsorption, thermal and thermo-catalytic oxidation [1,2].

VOCs can be removed by simple physisorption onto a high surface area support, in general carbon. Even though this process is relatively simple, disposal of spent carbon has to be carried out by thermal treatment. During the thermal treatment

toxic compounds can be liberated into the atmosphere. In the case of thermal oxidation, VOCs are oxidized at high temperatures, in the range 700–900 °C. Since this technique demands continuous supply of external heat energy, the use of a catalyst is proposed, which decreases the operating temperature to 300–500 °C. Various heterogeneous catalysts have been used to abate diluted VOCs. Catalytic techniques use less heat energy as compared to thermal oxidation and completely oxidize VOCs. However, catalytic techniques have limitations related to the energy supply at low VOC concentrations. Conventional techniques for the cleaning of dilute gas streams work efficiently only when the VOC concentration is higher than 1000 ppm, since in this case they are carried out in an auto-thermal regime [1,3].

An alternative approach to these conventional techniques is to use non-thermal (non-equilibrium) plasma (NTP), generated at atmospheric pressure. Destruction of diluted VOCs by applying NTP is of particular importance from the point of energy saving [5]. The NTP generates high energy electrons

* Corresponding author. Tel.: +41 21 693 31 82; fax: +41 21 693 31 90.

E-mail address: liubov.kiwi-minsker@epfl.ch (L. Kiwi-Minsker).

with short residence times capable of initiating chemical reactions at ambient temperature [3,4,6–9].

The NTP technique has been employed successfully for the destruction of various toxic VOCs like chlorinated and fluorinated hydrocarbons [10–12], inorganic pollutants such as SO₂, H₂S and NO_x [13–17] and also aliphatic [18–20] and aromatic hydrocarbons [2,3,20–24]. In the later case the total oxidation to CO₂ and H₂O is desired, but generally this aim is not achieved. The efficiency of NTP reaction can be envisaged based on two factors, either reducing power consumption, or suppressing the undesired by-product formation. Among the possible alternatives to improve the efficiency of the NTP reaction, increasing the residence time of VOCs in the plasma zone without changing the reactor size and the input energy seems to be a promising approach [20–26]. A combination of heterogeneous catalyst and non-thermal plasma appears to be the best choice for this task, where an increase in the residence time of the adsorbate molecules in the plasma zone can lead to improved selectivity towards total oxidation [4,25,26]. In practice, a catalyst can be combined with NTP in two ways: by introducing the catalyst in the discharge zone (in-plasma catalytic reactor, IPCR) or by placing the catalyst after the discharge zone (post-plasma catalytic reactor, PPCR). The better performance of the plasma catalytic technique is attained with the catalyst placed after the discharge zone. A strong deactivation of the catalysts has been reported when the catalyst is placed in the discharge zone [25,26].

However, a synergy between NTP and catalysts is expected by direct introduction of the catalyst in the discharge zone [4,25,26]. Most of the chemically active species generated in the plasma are short-lived and cannot reach the catalyst surface in downstream configuration. Hence, there is a need to modify the NTP reactor configuration in order to exploit the potential of the plasma catalytic technique.

Recently, catalytic filters based on sintered metal fibers (SMF) coated with oxides have been successfully used for the oxidation of VOCs [27,28]. These materials are multifunctional and capable of carrying out heat-exchange and particulate removal besides catalysis and exhibit good thermal and electrical conductivity [27,28]. In the present study a novel dielectric barrier discharge reactor is presented based on SMF. It has been designed and tested at atmospheric pressure and room temperature for the oxidation of toluene as a model VOC.

The catalyst combined with plasma was investigated for this purpose and various parameters like toluene concentration, catalyst composition, discharge voltage and frequency were systematically studied.

2. Experimental

2.1. Experimental set-up

The experimental set-up is shown in Fig. 1. Toluene was introduced with a motor-driven syringe pump and was diluted by a stream of air. The air flow rate was fixed at 500 ml/min (STP) with a mass flow controller (MFC). Toluene was mixed with air in a mixing chamber, which was electrically heated. The input concentration was varied between 100 and 1000 ppm by adjusting the flow rate of toluene. Air containing toluene was fed into the plasma reactor with a Teflon tube. The toluene concentration at the outlet was measured with a gas chromatograph (Shimadzu 14 B) equipped with a FID and a SP-5 capillary column (50 m length, 0.32 mm diameter and 0.5 μm film thickness). The formation of CO₂ and CO during toluene oxidation was simultaneously measured by using an infrared gas analyzer (Siemens Ultramat 21-P). As the volume changes due to chemical reactions are negligible, the selectivities to CO, CO₂ and CO_x can be stated as:

$$S_{\text{CO}} = \frac{[\text{CO}]}{7([\text{toluene}]_0 - [\text{toluene}])}$$

$$S_{\text{CO}_2} = \frac{[\text{CO}_2]}{7([\text{toluene}]_0 - [\text{toluene}])}$$

$$S_{\text{CO}_x} = S_{\text{CO}} + S_{\text{CO}_2}$$

where [CO] and [CO₂] are the outlet concentrations of CO and CO₂, respectively, and [toluene]₀ and [toluene] are the initial and final toluene concentrations. As it will be shown below, since there was no other hydrocarbon except toluene at the outlet, S_{CO_x} also represents the mass balance towards gaseous products. Ozone formed in the plasma reactor was measured with an UV absorption ozone monitor (API-450 NEMA). In order to ensure the formation of transition metal oxides on metal fibers and also to analyze the carbon deposit, XPS analysis of metal filters was carried out using an Axis Ultra

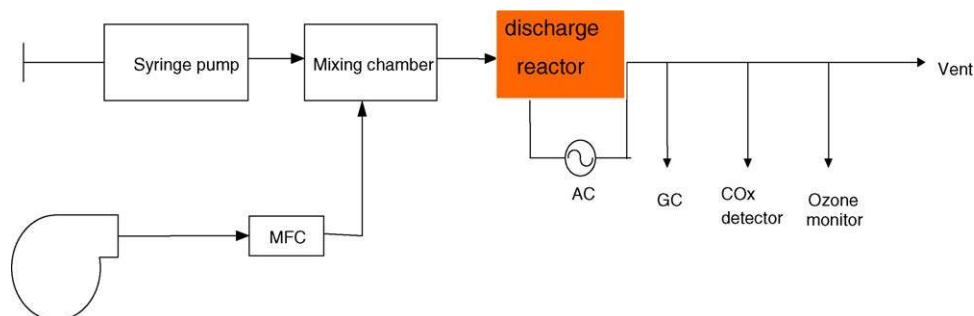


Fig. 1. Experimental set-up.

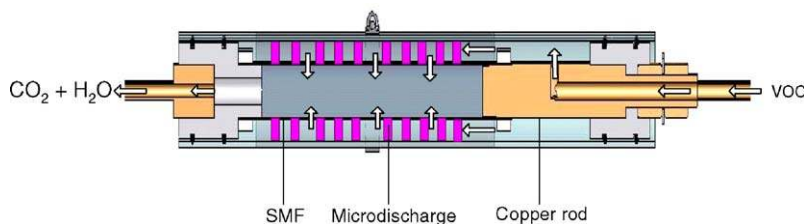


Fig. 2. Scheme of the plasma reactor.

ESCA system (Kratos, Manchester) with monochromated Al $K\alpha$ radiation (1486.6 eV).

2.2. Catalyst materials

Sintered metal fiber filters (Southwest Screens & Filters SA, Belgium) made of stainless steel (hereafter denoted as SMF) (Cr 16–18; Ni 10–13; Mo 2–2.5; C < 0.01; Fe balance) in the form of a uniform pore panel (0.29 mm thick, 80% porosity, 675 g/m^2) were used as the inner electrode. This material consists of thin uniform metal fibers with diameter $\sim 20 \mu\text{m}$ and porosity of $\sim 80 \text{ wt}\%$. For the deposition of 3 wt% MnO_x and CoO_x , the SMF (stainless steel filter) was first oxidized at $600 \text{ }^\circ\text{C}$ for 3 h, followed by impregnation with Co and Mn nitrate aqueous solutions of desired concentrations. Drying at room temperature and calcination at 773 K in air for 5 h renders metal oxide catalytic film supported on SMF. Finally, SMF filters were subjected to an electrical hot press treatment to shape them in cylindrical form with a diameter of 11.5 mm.

3. Results

3.1. Plasma reactor

The dielectric barrier discharge (DBD) reactor is shown in Fig. 2. The discharge was generated in a cylindrical quartz tube with an inner diameter of 18.5 mm and wall thickness of 1.6 mm. Silver paste was painted on the outer surface of the quartz tube, acting as the outer electrode, whereas the SMF in the form of a cylindrical tube served as the inner electrode and also as the catalyst. The latter property is the main novelty of

the reactor. The discharge length was 10 cm and the discharge gap was around 3.5 mm. One end of the SMF catalytic electrode was connected through a copper rod to AC high voltage, whereas the other end was connected to the inlet gas stream through a Teflon tube. The electrical discharge was ignited by applying AC high voltage in the range 12.5–22.5 kV (peak-to-peak), supplied by an amplifier and a function generator (Vareg, Switzerland) in the frequency range 200–450 Hz. The gas after passing the discharge zone diffuses through the SMF and was analyzed with a gas chromatograph at the outlet. Conversion of toluene at each applied voltage was measured after 30 min. Experiments were also carried out by replacing SMF with conventional copper electrode.

The voltage–charge (V – Q) Lissajous method was used to determine the discharge power in the plasma reactor. The charge Q (i.e. current integrated over time) was measured from the voltage across a capacitor of 100 nF connected in series to the ground electrode. The applied voltage was measured with a 1000:1 high voltage probe (Luke 80 K-40 HV). The voltage and charge waveforms were recorded by a digital oscilloscope (Tektronix, TDS 3054), by averaging 256 scan and plotted to obtain a typical Lissajous diagram as shown in Fig. 3.

3.2. Discharge characterization

Fig. 3a and b represent typical V – Q Lissajous figures for 22.5 and 17.5 kV at a frequency 350 Hz. The area of the Lissajous figure characterizes the energy dissipated after applying one working voltage period. The average power (W) dissipated in the discharge was calculated by multiplying the area by the frequency and the capacitance [7,23]. The specific

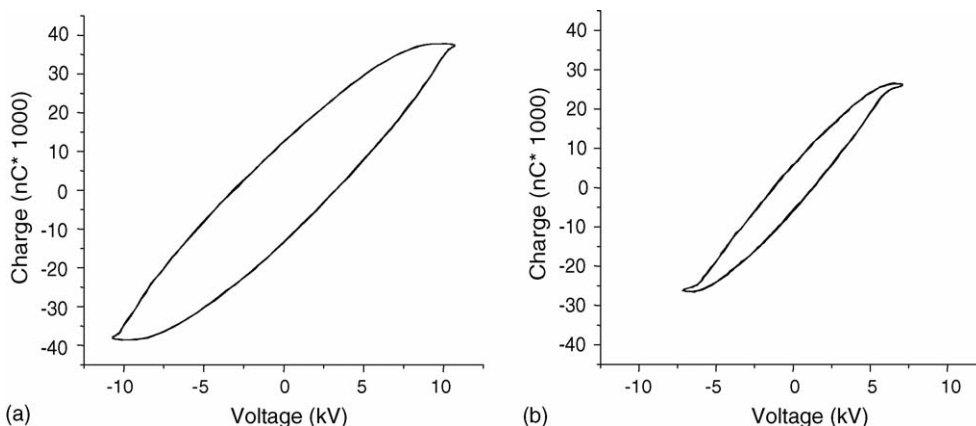


Fig. 3. V – Q Lissajous figure of the plasma reactor for frequency 350 Hz and voltage: (a) 22.5 kV and (b) 17.5 kV.

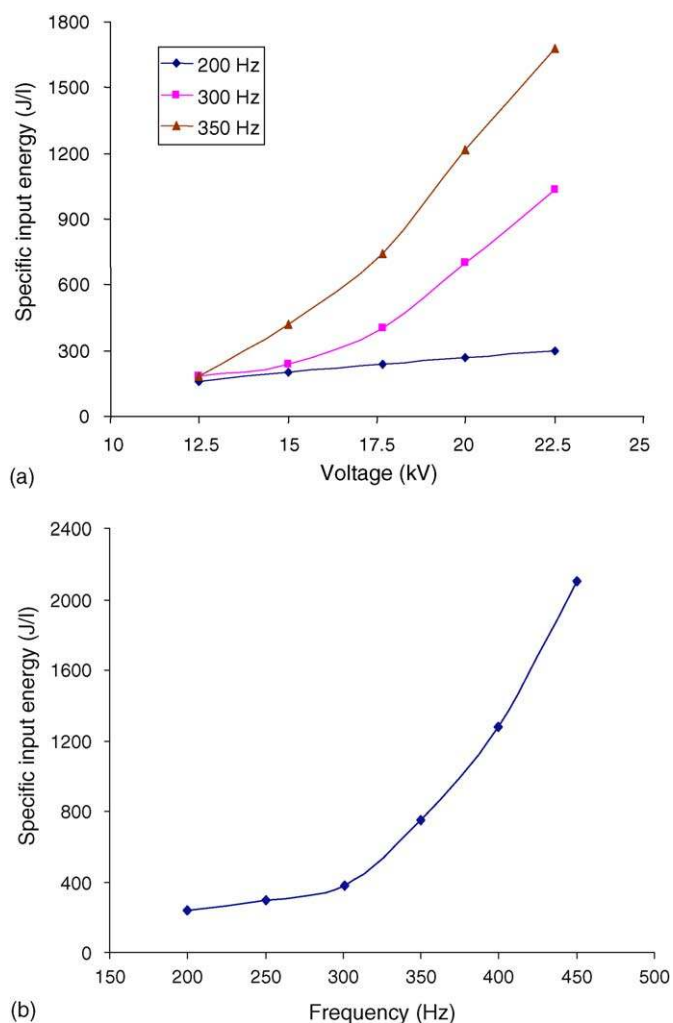


Fig. 4. Variation of the specific input energy (SIE) as a function of (a) voltage and frequency and (b) frequency at a constant voltage of 17.5 kV.

input energy (SIE) of the discharge was calculated using the relation:

$$\text{Specific input energy (J/l)} = \frac{\text{discharge power(W)}}{\text{gas flow rate(l/s)}}$$

As seen from Fig. 3, increasing the applied voltage at a constant frequency increases the power and the specific input energy (Fig. 4a). For example, at 200 Hz, the SIE increased from 160 J/l (12.5 kV) to 295 J/l (22.5 kV). When the frequency was increased to 300 Hz, a considerable increase up to 1030 J/l was observed (Fig. 4a). If the frequency is further increased to 350 Hz, the SIE reached a maximum of 1650 J/l at 22.5 kV. In a similar way, increasing the frequency at a constant voltage also increases the SIE. Fig. 4b represents the variation of SIE as a function of frequency in the range of 200–450 Hz at a constant voltage of 17.5 kV. As seen, SIE is proportional to the frequency and reached a maximum of 2100 J/l at 450 Hz.

As stated above, the plasma reaction would be energetically feasible for the VOC destruction only with a low consumption of energy. Therefore, during the present study, toluene

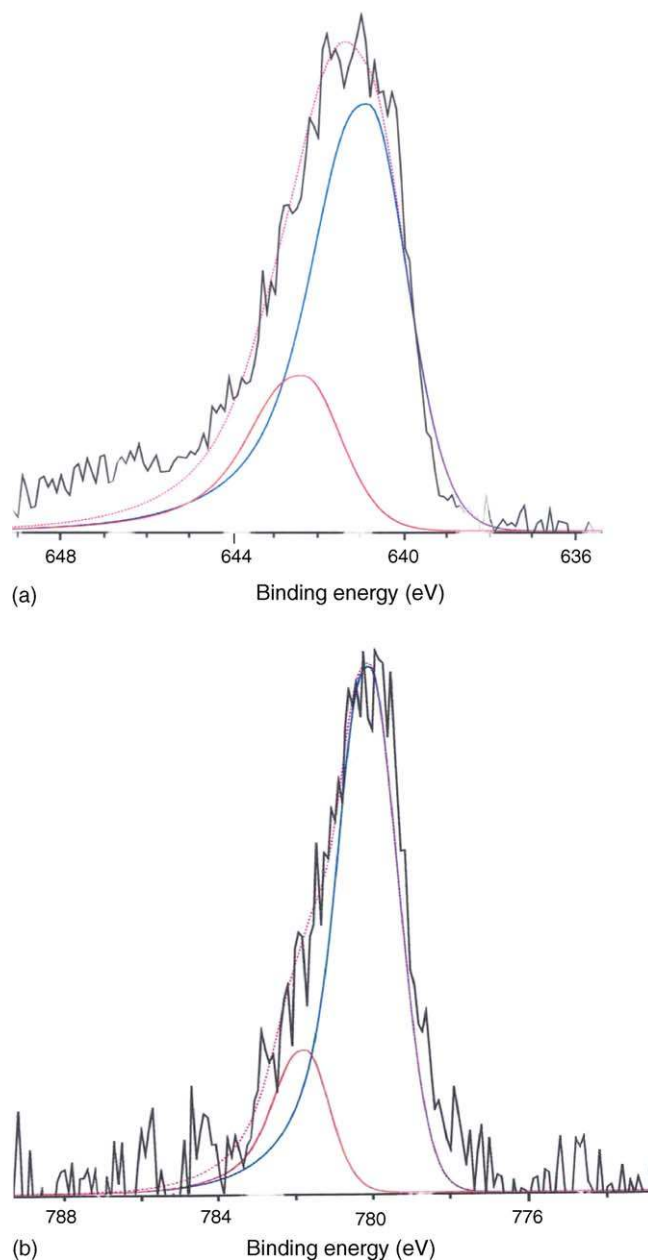


Fig. 5. XP spectrum of the 2p region of (a) MnO_x/SMF and (b) Co/SMF.

destruction was carried out with the SIE < 295 J/l. This SIE is nearly three times lower as compared to the energy required during the thermal destruction (~1000 J/l).

3.3. Characterization of Mn and Co oxide catalysts by XPS

In order to confirm the formation of Mn and Co oxides on SMF surface, XPS was used (Fig. 5a and b). The deconvolution of Mn 2p in 638–648 eV region shows two peaks at 640.8 and 642.3 eV correspond to the +2 and +4 oxidation states, respectively (Fig. 5a). In a similar manner, the XP spectra of CoO_x/SMF in the Co 2p region also show two peaks in 776–784 eV regions (Fig. 5b). The first peak, centered on 779.9 eV, was assigned to Co in the mixed valence state between +2 and

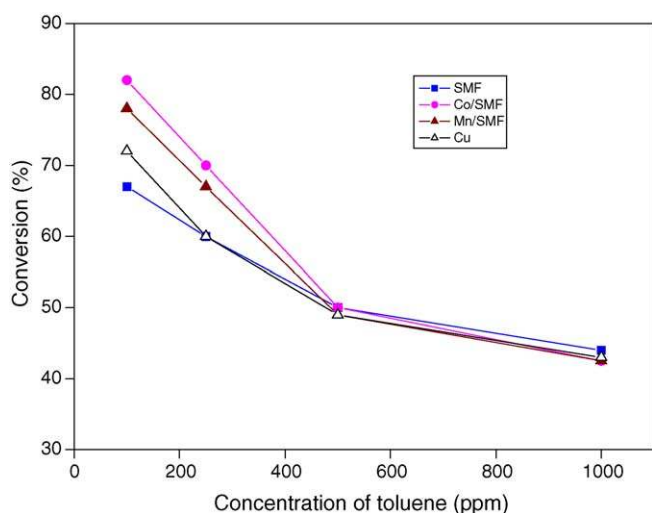


Fig. 6. Effect of the initial toluene concentration on the performance of the plasma reactor at SIE 160 J/l (12.5 kV, 200 Hz).

+3 (Co_3O_4), whereas a second peak, centered on 781.7 eV, was assigned to Co in the +2 oxidation state ($\text{Co}(\text{OH})_2$). This is in agreement with the observations made earlier during the synthesis of CoO_x/SMF [28,29].

3.4. Influence of initial concentration of toluene on the reactor performance

Fig. 6 shows the conversion of toluene as a function of its initial concentration between 100 and 1000 ppm. These experiments were carried out at a constant voltage (12.5 kV) and frequency (200 Hz), corresponding to a SIE of 160 J/l. The inner electrode was either a conventional Cu electrode, or the catalytic SMF electrode. The conversion of toluene decreases with increasing toluene concentration. In the DBD reactor using a Cu electrode, the removal efficiency for 100 ppm of toluene at a SIE of 160 J/l was ~70%, and decreased to ~45% for a toluene concentration of 1000 ppm. A similar trend in the toluene conversion was observed for the DBD reactor with the SMF catalytic electrodes.

Fig. 7a shows the selectivity to CO_x ($\text{CO}_2 + \text{CO}$) as a function of toluene inlet concentration (100–1000 ppm) at 160 J/l (12.5 kV and 200 Hz frequency). No other hydrocarbon except toluene was detected in the effluent gas. Since CO_2 and CO are the only gaseous products formed, the solid deposited on the walls of the reactor completes the total carbon content. Hence, as shown in Fig. 7a, for 100 ppm of toluene at SIE 160 J/l, on the SMF and Cu electrode nearly 70% of toluene was oxidized to gaseous products, whereas for 1000 ppm, only 30% was gasified and the rest (~70%) was converted to an undesired solid carbon deposit on the catalyst surface. Fig. 7b shows the selectivity to CO_2 as a function of toluene inlet concentration: for 100 ppm of toluene, the Cu electrode showed ~25% selectivity to CO_2 and it dropped to ~10% for 1000 ppm of toluene. Metal oxides (Mn, Co) supported on SMF increased the selectivity to CO_2 especially for toluene concentration ≤ 400 ppm. For example, during the destruction of 100 ppm of toluene, the metal oxide supported SMF catalytic electrode

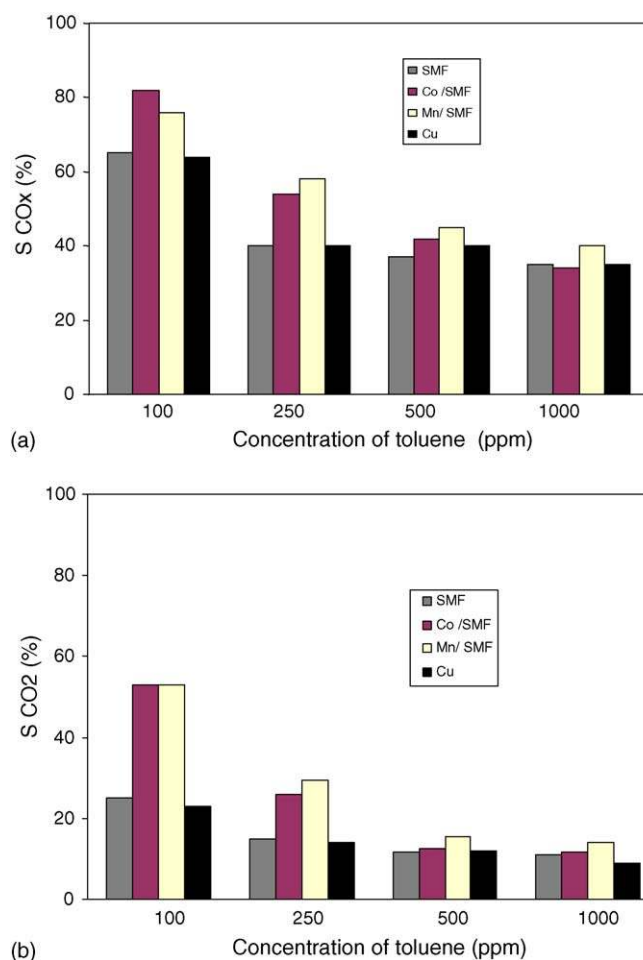


Fig. 7. Effect of the initial toluene concentration on (a) selectivity to CO_x and (b) selectivity to CO_2 at SIE 160 J/l (12.5 kV, 200 Hz).

showed ~50% selectivity to CO_2 against 25% selectivity when using a Cu electrode in DBD reactor. Further studies were carried out with toluene concentration of 100 ppm to screen and optimize the SMF catalytic electrode.

3.5. Influence of the Mn and Co oxides supported on SMF electrode on the efficiency of toluene destruction in DBD reactor

For the initial concentration of toluene ≤ 400 ppm, an increase in the conversion of toluene was observed when the catalytic SMF electrode modified by CoO_x and MnO_x was used. At SIE of 160 J/l (12.5 kV and 200 Hz) with MnO_x/SMF catalyst, for 100 ppm of toluene, a conversion ~80% was obtained against 70% on non-modified SMF electrode (Fig. 8). A similar effect was also observed with CoO_x/SMF , since using the same experimental conditions a conversion of toluene ~80% was obtained. The selectivity to CO_x was also higher with CoO_x/SMF (80%) and MnO_x/SMF (75%) electrodes as compared to SMF (65%). Important is that the selectivity to CO_2 increased to 50% with CoO_x and MnO_x/SMF as compared to 25% on SMF electrode. The presence of ozone may play an important role when CoO_x and MnO_x/SMF electrodes were used. Interaction of ozone with metal oxide catalysts leads to

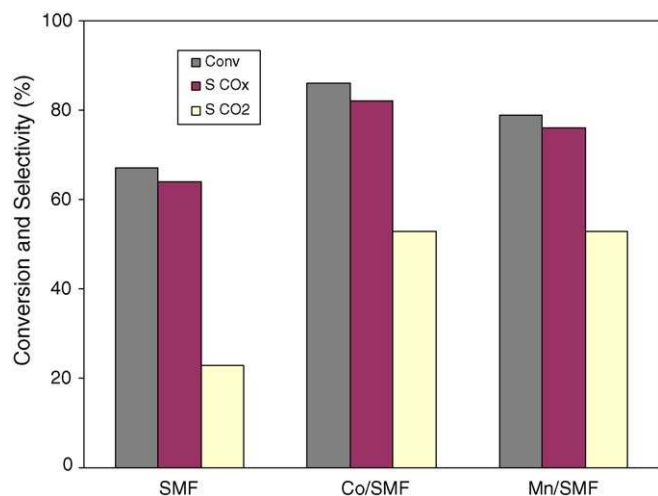


Fig. 8. Influence of the metal oxide on the conversion of toluene and product formation at 160 J/l (100 ppm toluene, 12.5 kV, 200 Hz).

the formation of reactive atomic oxygen species from ozone molecule [22,30]. This can explain the better performance of CoO_x and MnO_x/SMF catalytic electrodes. Similar observations were earlier made when the addition of MnO_x catalyst to the plasma reactor was observed to increase its efficiency [22]. However, during the present study, the influence of other short-lived species formed due to plasma cannot be ruled out. For 100 ppm of the inlet toluene concentration, at low SIE 160 J/l (12.5 kV and 200 Hz) the undesired products formation was minimized. The selectivity to gaseous products, S_{CO_x} ~ 80% was attained with high selectivity for toluene oxidation to CO₂ (S_{CO₂} ~ 50%) on MnO_x/SMF.

3.6. Effect of applied voltage on the destruction of toluene

Conversion of 100 ppm toluene was measured at a voltage between 12.5 and 22.5 kV and a constant frequency of 200 Hz.

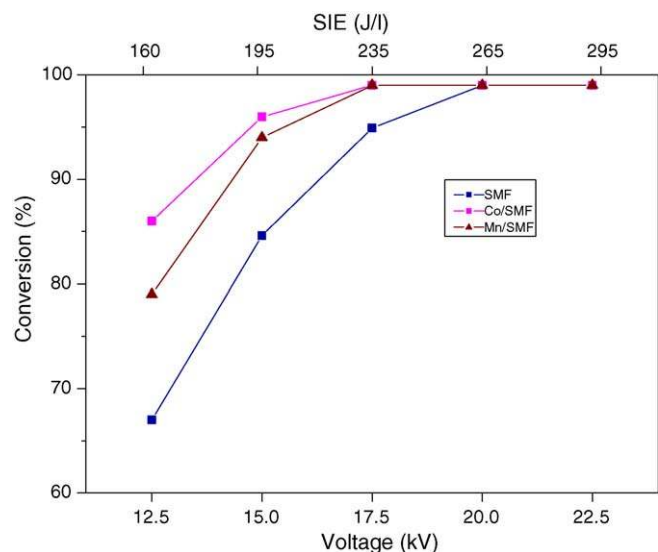


Fig. 9. Effect of the applied voltage on the destruction of toluene over different catalytic electrodes (100 ppm, 200 Hz).

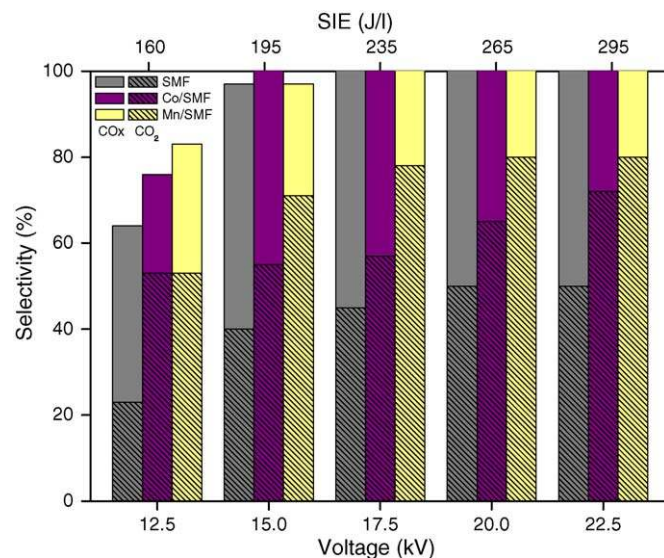


Fig. 10. Effect of the applied voltage on the selectivity to CO_x and CO₂ (100 ppm toluene, 200 Hz).

These conditions correspond to the SIE of 160 and 295 J/l, respectively. The results are presented in Fig. 9. Conversion increases with the applied voltage in all cases. With the SMF electrode, the toluene conversion reaches 100% at 20 kV (265 J/l), while with Co and Mn oxides supported on SMF, it was achieved even at 17.5 kV (SIE of 235 J/l). As mentioned in the earlier section, this difference may be due to the interaction of ozone with the metal oxide catalyst leading to the formation of atomic oxygen [22,30].

It is well known that in plasma catalytic techniques, the main problem is due to the deposition of solid by-products on the electrodes. As seen from Fig. 10, in the DBD reactor with all the catalytic electrodes, during the destruction of 100 ppm of toluene no carbon deposit was observed (~100% selectivity to CO_x) with voltage higher than 15 kV (SIE 195 J/l). Fig. 10 also represents the selectivity to CO₂ for various catalysts during destruction of 100 ppm of toluene, which also increases with increasing applied voltage. Toluene was completely converted to gaseous products. With the SMF electrode, the selectivity to CO₂ increases with applied voltage and reaches a maximum of ~50%. However, the CO₂ selectivity increased on CoO_x and MnO_x/SMF electrodes. Even at 12.5 kV (160 J/l), CoO_x/SMF shows ~50% selectivity and reaches 70% at 22.5 kV. MnO_x/SMF shows a better performance, where the selectivity to CO₂ reaches nearly 80% even at 17.5 kV.

4. Conclusions

1. A novel dielectric barrier discharge reactor was designed, where the catalyst made of sintered metal fibers was used as the inner electrode.
2. This reactor demonstrated high efficiency at low input energy (235 J/l) showing complete conversion during the destruction of 100 ppm of toluene against the energy required for the thermal destruction (~1000 J/l).

3. MnO_x and CoO_x supported on the SMF catalytic electrode improved the performance of the plasma DBD reactor up to ~80% selectivity to total oxidation products (CO_2 and H_2O). Hence, the novel DBD catalytic reactor demonstrated promising performance and is suitable for the abatement of low content VOC.

Acknowledgements

The authors acknowledge the Swiss National Science Foundation (“SCOPES” program) and the Swiss Commission of Technology and Innovation (CTI, Bern) for the financial support.

References

- [1] R.G. McInnes, Chem. Eng. Prog. (1995) 36.
- [2] Y.H. Song, S.J. Kim, K. Choi, T. Yamamoto, J. Electrostat. 55 (2002) 189.
- [3] M. Magureanu, N.B. Mandache, P. Eloy, E.M. Gaigneaux, V.I. Parvulescu, Appl. Catal. B: Environ. 61 (2005) 13.
- [4] F. Holzer, U. Roland, F.D. Kopinke, Appl. Catal. B: Environ. 38 (2002) 163.
- [5] T. Oda, J. Electrostat. 57 (2003) 293.
- [6] A. Bogaerts, E. Neyts, R. Gijbels, J. Mullen, Spectrochim. Acta B57 (2002) 609.
- [7] M. Kraus, B. Eliasson, U. Kogelschatz, A. Wokaun, Phys. Chem. Chem. Phys. 81 (2001) 294.
- [8] K.L.L. Vercammen, A.A. Berezin, F. Lox, J.S. Chang, J. Adv. Oxid. Tech. 2 (1997) 312.
- [9] X. Xu, Thin Solid Films 390 (2001) 237.
- [10] B. Penetrante, M.C. Hsiao, J.N. Bardsley, B.T. Merrit, G.E. Vogtlin, A. Kuthi, C.P. Burkhart, J.R. Bayless, Plasma Sources Sci. Technol. 6 (1997) 251.
- [11] T. Yamamoto, I.K. Mizuno, I. Tamori, A. Ogata, M. Nifuku, M. Michalska, G. Prieto, IEEE Trans. Ind. Appl. 32 (1996) 100.
- [12] M.B. Chang, H.M. Lee, Catal. Today 89 (2004) 109.
- [13] A. Gal, M. Kurahashi, M. Kuzumoto, J. Phys. D: Appl. Phys. 32 (1999) 1163.
- [14] K. Kiyokawa, H. Matsuoaka, A. Itou, K. Hasegawa, K. Sugiyama, Surf. Coat. Technol. 112 (1999) 25.
- [15] R. Li, Y. Keping, J. Miao, X. Wu, Chem. Eng. Sci. 53 (1998) 1529.
- [16] M.J. Kirkpatrick, W.C. Finney, B.R. Locke, Catal. Today 89 (2004) 117.
- [17] A. Czernichowski, NATO ASI Ser. A G34 (1993) 371.
- [18] C. Ayrault, J. Barrault, N. Blin-Simiand, F. Jorand, S. Pasquiers, A. Rousseau, J.M. Tatibouet, Catal. Today 89 (2004) 75.
- [19] S. Futamura, A. Zhang, G. Prieto, T. Yamamoto, IEEE Trans. Ind. Appl. 34 (1998) 967.
- [20] V. Demidiouk, S.I. Moon, J.O. Chae, Catal. Commun. 4 (2003) 51.
- [21] A. Ogata, K. Mizuno, S. Kushiyaama, T. Yamamoto, Plasma Chem. Plasma Process. 19 (1999) 383.
- [22] S. Futamura, H. Einaga, H. Kabashima, L.Y. Jwan, Catal. Today 89 (2004) 89.
- [23] H.H. Kim, S.M. Oh, A. Ogata, S. Futamura, Appl. Catal. B: Environ. 56 (2005) 213.
- [24] H. Einaga, T. Ibusuki, S. Futamura, IEEE Trans. Ind. Appl. 37 (2001) 1476.
- [25] U. Roland, F. Holzer, F.D. Kopinke, Appl. Catal. B: Environ. 58 (2005) 217.
- [26] U. Roland, F. Holzer, F.D. Kopinke, Appl. Catal. B: Environ. 58 (2005) 227.
- [27] I. Yuranov, A. Renken, L. Kiwi-Minsker, Appl. Catal. A: Gen. 281 (2005) 55.
- [28] I. Yuranov, L. Kiwi-Minsker, A. Renken, Appl. Catal. B: Environ. 43 (2003) 217.
- [29] N. Dunand, Diploma Thesis, EPFL (1999) 1.
- [30] W. Li, G.V. Gibbs, S.T. Oyama, J. Am. Chem. Soc. 120 (1998) 9041.